Available online at www.sciencedirect.com
ScienceDirect
Thermochimica Acta 451 (2006) 16–21
thermochimica acta
www.elsevier.com/locate/tca

# Effects of anion substitution on the acid properties of hydroxyapatite

Neuman S. Resende, Marcio Nele, Vera M.M. Salim *

*Programa de Engenharia Química, COPPE/Universidade Federal do Rio de Janeiro, Centro de Tecnologia, Bl.G/115, Ilha do Fundão, 21.945-970 Rio de Janeiro, RJ, Brazil*

Received 18 May 2006; received in revised form 14 August 2006; accepted 15 August 2006
Available online 30 August 2006

**Abstract**

The influence of the anionic substitution and the thermal treatment on the acid/base properties of hydroxyapatite was studied by temperature-programmed desorption of ammonia (TPD-$NH_3$). Stoichiometric hydroxyapatite, A-type and B-type carboapatites have been synthesized. Substitution of $OH^-$ by the $CO_3^{2-}$ (Carbo-A) modifies the acid strength distribution, increases the overall acidity and acid site density ($\mu mol/m^2$). Substitution of the $PO_4^{3-}$ (B-site) by the $CO_3^{2-}$ did not lead to noticeable changes on the adsorption sites. These results suggest that the $Ca^{2+}$ ions are the most significant sites for ammonia adsorption.


*Keywords:* Carboapatites; Hydroxyapatite; TPD-$NH_3$; Anionic substitution; Thermal treatment

## 1. Introduction

The synthetic apatites, widely used initially as bioceramic materials, are also studied as potential adsorbants for heavy metals [1,2] and have been applied as catalysts in various transformations. Hydroxyapatite is a catalyst for gas-phase acid/base reactions [3–6], gas-phase partial oxidation reactions [7–10] and in many liquid phase reactions such as Knoevenagel reactions [11], hydration of nitriles [12] and Friedel–Crafts alkylation [13].

Hydroxyapatite $Ca_{10}(PO_4)_6(OH)_2$ – HAp – may present significant differences in surface and bulk properties, even in materials with very close chemical compositions due to cation/anion substitution or to variation on the material stoichiometry. Calcium deficient HAp, with the general formula $Ca_{10-x}(HPO_4)_x(PO_4)_{6-x}(OH)_{2-x}$ $[0 \leq x \leq 1]$ presents different catalytic performance from stoichiometric apatites. The stoichiometric apatites ($x = 0$) are predominantly basic solids, while the non-stoichiometric also contain acid sites [5,14].

Calcium substitution allows the addition of metallic sites to the material rendering it active in methane activation reactions; anion substitution reactions, $PO_4^{3-}$ groups by $HPO_4^{2-}$ and $CO_3^{2-}$, and $OH^-$ by $F^-$, modify the surface properties and the thermal stability of the material [15].

The apatite structure possesses a great flexibility in accepting substitutions in its network and substitutions of calcium ions ($Ca^{2+}/M^{2+}$) [16]. The structure of calcium hydroxyapatite, first resolved by Naray-Szabo [17] and later refined by Beevers and McIntyre [18], is presented in Fig. 1. The framework of stoichiometric calcium hydroxyapatite can be described as a compact assemblage of tetrahedral $PO_4$ groups where each $PO_4$ tetrahedron is shared by one column, and delimit two types of unconnected channels. The first channel has a diameter of 2.5 Å and is bordered by $Ca^{2+}$ ions (denoted Ca (I)). The second type plays an important role in the properties of the apatites. It has a diameter of around 3.5 Å and is also delimited by oxygen and $Ca^{2+}$ ions in a coordination of 7 (denoted Ca (II)). These channels host OH groups (or halide ions) along the *c* axis to balance the positive charge of the matrix. The existence of two different calcium sites is of special interest because the material properties can be tuned by the specific site modified [19]. The $OH^-$ ions are located in columns perpendiculars to the unit cell face, at the center of the hexagon formed by groups of coplanar calcium ions. The oxygen of the hydroxyl group is located 0.4 Å out of the plane formed by the calcium ion, and hydrogen 1 Å farther, almost on the triangle plane of calcium. The environment around the $OH^-$ sites is very attractive for substitutions because it allows one to control not only the site acid strength but also the ratio between Lewis and Brönsted acid sites.

* Corresponding author.
*E-mail address:* vera@peq.coppe.ufrj.br (V.M.M. Salim).

0040-6031/$ – see front matter © 2006 Elsevier B.V. All rights reserved.
doi:10.1016/j.tca.2006.08.012

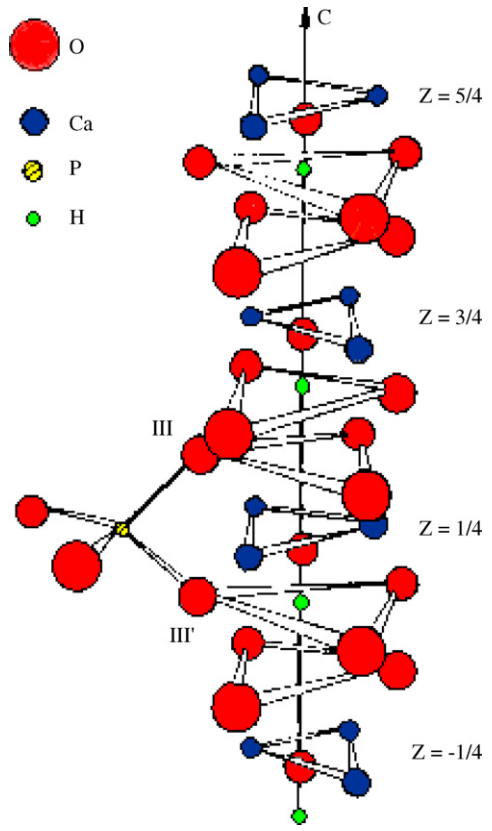


Fig. 1. The structure of calcium hydroxyapatite.

In the case of carboapatites, $Ca_{10-x/2}[(PO_4)_{6-x}(CO_3)_x][(OH)_{2-2y}(CO_3)_y]$, the carbonate ion can be located at two different sites, depending on the temperature that the material is prepared [20]. If the material is synthesized at high temperatures (~900 °C), the carbonate ion substitutes only the hydroxyl ion (A site), originating a Carbo type A apatite. If the material is prepared at low temperatures (~400 °C) and by precipitation, the substitution is less selective and both hydroxyl (A site) and phosphate ions (B site) are replaced, and a Carbo type B apatite is formed [19,21].

The possibility of controlling the material stoichiometry and precise ion substitutions make the hydroxyapatite a very attractive material for structure–property investigations, especially the development of catalysts with designed properties.

The acid properties of a solid are related to the number of acid sites and their strength. The solid surface is intrinsically heterogeneous, and structural/non-stoichiometric defects generate a very broad acid site distribution that is very difficult to be precisely characterized. Nevertheless, the thermo-programmed desorption (TPD) of ammonia can give a quantitative understanding of the total amount of acidity and a qualitative picture of the strength of the acid sites [22].

This work presents a study of the effects of anion substitutions and different calcination procedures on the acid site strength distribution of the apatites. These treatments change significantly the acid properties of the solid, including overall acid strength, acid sites distribution and ratio of Lewis to Brönsted acid sites.

## 2. Experimental

### 2.1. Apatite synthesis

#### 2.1.1. Hydroxyapatite

The hydroxyapatite precursor was prepared by slowly adding a 0.3 M $(NH_4)_2HPO_4$ aqueous solution to a 0.5 M $Ca(NO_3)_2{\cdot}4H_2O$ aqueous solution, both alkalinized by adding $NH_4OH$ (pH 10–11), at 80 ± 5 °C under continuous stirring. The mother suspension was aged at the precipitation temperature for 2 h. The precipitated was then washed several times with hot water (80 °C) to eliminate any residual alkali. After filtration, the obtained solid was dried in an oven at 80 °C for 24 h. This precursor was called (HAp-dried). A portion of the dried precursor was calcined at 900 °C for 5 h and sieved at 65 mesh, this material was named (HAp-calc).

#### 2.1.2. Carboapatite A

The calcined hydroxyapatite (HAp-calc) was subsequently treated at 900 °C, under $CO_2$ flow (high-purity, 99.99%) for 10 h. Then, the material was allowed to cool down under $CO_2$ flow. The obtained material was labeled Carbo-A, contained around 5% (w/w) of carbonate ions.

#### 2.1.3. Carboapatite B

An alternative procedure was followed for the synthesis of the hydroxyapatite, it was prepared an aqueous solution containing 0.24 M of $(NH_4)_2HPO_4$ and 0.12 M of $(NH_4)_2CO_3$ in order to obtain 10% (w/w) of carbonate ions in the final solid. This solution was also slowly added to a 0.5 M $Ca(NO_3)_2{\cdot}4H_2O$ aqueous solution, both alkalinized by adding $NH_4OH$ (pH 10–11), at 80 ± 5 °C under continuous stirring. The mother suspension was aged at the precipitation temperature for 2 h. The precipitate was then washed several times with hot water (80 °C) to eliminate any residual alkali. After filtration, the obtained solid was dried in an oven at 80 °C for 24 h. The dried material was calcined at 400 °C for 3 h and sieved at 65 mesh. The obtained material was labeled Carbo-B, contained around 12% of carbonate ions (w/w) and the degree of substitution of phosphate ions obtained was around 17%.

### 2.2. Characterization

X-ray powder diffraction (XRD) patterns of the samples were recorded in a Rigaku X-ray diffractometer (Dmax 2200) equipped with a graphite monochromator using Cu Kα radiation (40 kV and 40 mA). The step-scans taken over the range of $2\theta$ from 5° to 130° in step of 0.05, the intensity data for each step was collected for 5 s. Lattice parameters were refined by Rietveld method and the structure refinements were performed with FULLPROF program [23]. The crystallite size was measured by Scherrer equation using selected peak widths from XRD patterns [24].

The specific surface area was measured by nitrogen adsorption at 77 K (BET method) using Micrometrics ASAP-200 equipment.

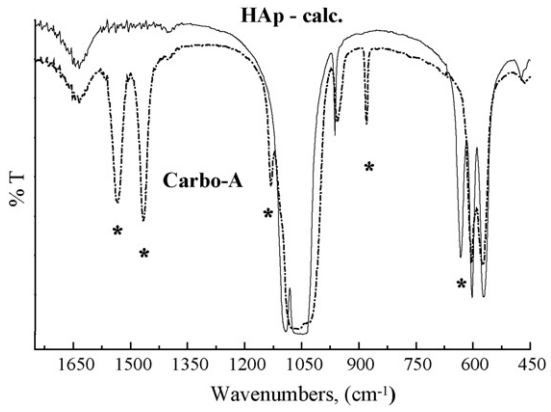


Fig. 2. FTIR spectra of the Carbo-A and calcined hydroxyapatite (HAp-calc).

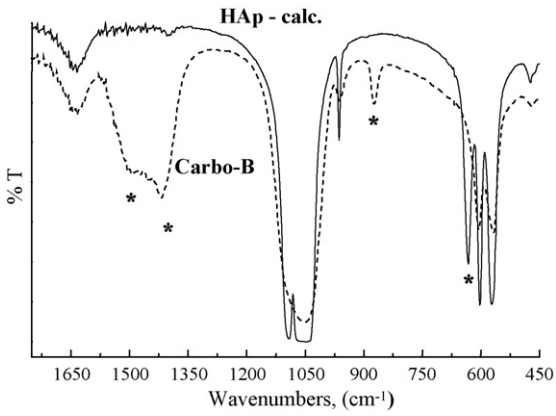


Fig. 3. FTIR spectra of the Carbo-B and calcined hydroxyapatite (HAp-calc).

Infrared spectra were obtained with Perkin-Elmer FTIR System 2000. The self-supported pellets were prepared with 35–50 mg of material, pre-treated at 200 °C and under vacuum ($10^{-5}$ Torr), for 1 h in a specially designed glass cell.

The thermo-programmed desorption (TPD) was carried out in a Micrometrics TPD/TPR 2900 equipment coupled with a quadrupole mass detector (Balzer QMS 200). The experimental conditions were a heating rate of 10 °C/min, final temperature of 1100 °C, sample mass of about 300 mg with helium as gas carrier (60 L/min). The sample was kept at 150 °C for 1 h under helium flow (60 mL/min), then the temperature was lowered to 70 °C and the flow was switched to a mixture of 4% $NH_3$/He (60 mL/min). The sample was maintained in 4% $NH_3$/He flow for 1 h, and then the flow was switched back to pure helium and the temperature program started. The desorbed compounds were monitored using the relation *m*/*e*: $NH_3$ (*m*/*e* = 15), NO (*m*/*e* = 30), $H_2O$ (*m*/*e* = 18), $N_2$ (*m*/*e* = 28), $O_2$ (*m*/*e* = 32, 16), $N_2O$ (*m*/*e* = 44). The total acidity was calculated by measuring the total ammonia uptake.

## 3. Results and discussion

The infrared spectra of the carboapatites A and B were compared to the calcined sample (HAp-calc) spectra. Carboapatite A (Fig. 2) shows three well defined bands originating from stretching vibrations of carbonate ions, due to the substitution of phosphate groups ($PO_4^{3-}$), at 879 $cm^{-1}$ ($\nu_2$), at 1465 $cm^{-1}$ ($\nu_{3a}$) and at 1534 $cm^{-1}$ ($\nu_{3b}$), for both substitution, $PO_4^{3-}$ groups (type B) and $OH^-$ groups (type A). These bands attributed to $CO_3^{2-}$ ions can also be seen in the Carboapatite B spectrum (Fig. 3), but shifted to a lower wavenumber: at 874 $cm^{-1}$ and a broad band with peaks at 1417 $cm^{-1}$ (type B) and at 1505 $cm^{-1}$, characteristic from type AB, with a shoulder at 1455 $cm^{-1}$ ($\nu_{3a}$) and at 1538 $cm^{-1}$ ($\nu_{3b}$) [25]. As reported by Elliott [19], the frequencies of ($\nu_2$) and ($\nu_{3a}$) are independent of the degree of substitution of $OH^-$ by $CO_3^{2-}$ ions within ±4 $cm^{-1}$, however $\nu_{3b}$ decreases without a clear pattern from about 1565 to 1527 $cm^{-1}$ as the degree of substitution increases. Infrared studies of substituted apatites [21] have shown that the frequency of $\nu_{3b}$ depends only on the hexagonal unit cell volume; as the volume increases, $\nu_{3b}$ decreases linearly.

The infrared spectroscopy is an important tool for characterizing apatites, in especial it allows one to easily identify the type of site substituted by the carbonate ion in the carboapatite framework. Regarding to the substitution, it is clear in both Figs. 2 and 3 that $OH^-$ group band from libration mode at 631 $cm^{-1}$ present in the HAp-calc sample is absent for carboapatite samples, indicating that all hydroxyl groups were replaced by carbonate ions.

More information about the structure can be obtained from the phosphate related bands (900–1200 $cm^{-1}$). The band at 1130 $cm^{-1}$, characteristics of the stoichiometric apatites containing $HPO_4^{2-}$ ion and carbonate $CO_3^-$, is intense for the carboapatite A. This band is absent in the carboapatite type B, suggesting that carbonate ions replace phosphate ions in the carboapatite type B, occupying the anionic trivalent sites ($PO_4^{3-}$).

The IR spectra showed that the $CO_3^{2-}$ ions are in two different environments and the crystal data obtained from XRD pattern (Fig. 4) confirmed the hexagonal lattice symmetry (space group $P6_3/m$) for all samples [19,20]. The calculated cell parameters derived from XRD data for the apatites prepared in this study are presented in Table 1.

Table 1
Cell parameters from XRD data for the apatites

| Samples | Chemical formulae | Structure | *Z* | Density | Lattice constants (Å) | | |
|---|---|---|---|---|---|---|---|
| | | | | | *a* | *b* | *c* |
| HAp-dried | $Ca_{10}(PO_4)_6(OH)_2$ | Hexagonal | 1 | 3.159 | 9.434 | *a* | 6.883 |
| HAp-calc | $Ca_{10}(PO_4)_6(OH)_2$ | Hexagonal | 1 | 3.159 | 9.430 | *a* | 6.885 |
| Carbo-A | $Ca_{10}(PO_4)_6(CO_3)$ | Hexagonal | 1 | 3.114 | 9.488 | *a* | 6.878 |
| Carbo-B | $Ca_{9.5}(PO_4)_5(CO_3)_2$ | Hexagonal | 1 | 3.096 | 9.355 | *a* | 6.906 |

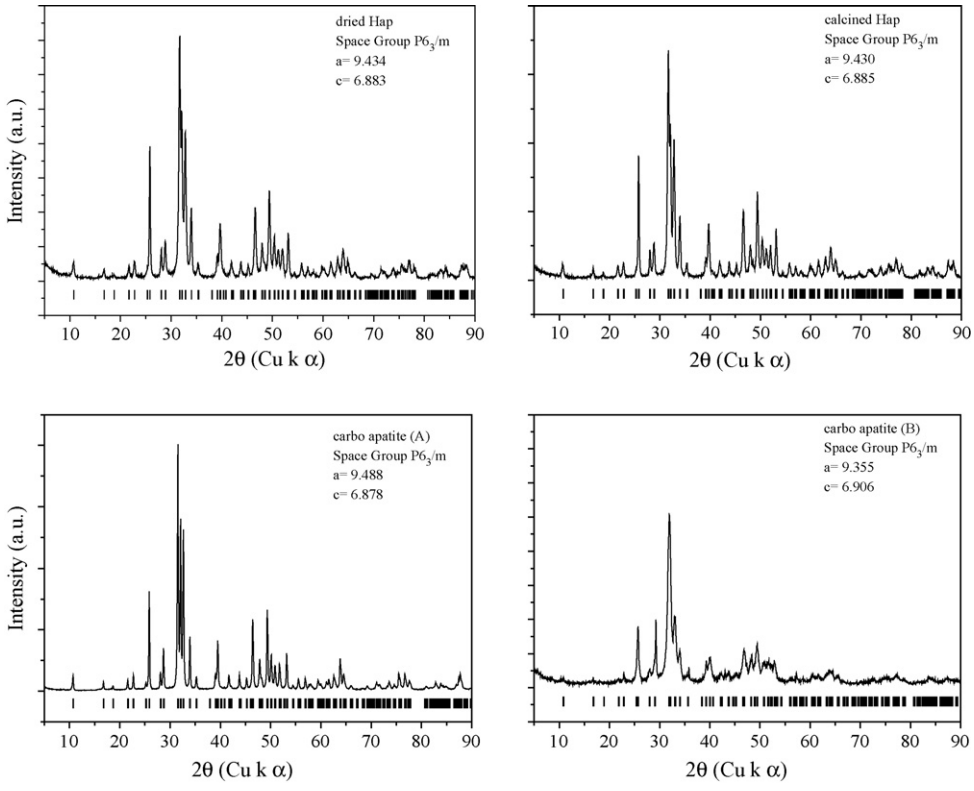


Fig. 4. XRD patterns for the apatites.

Table 2 presents the results of the surface area measurements, along with the total amount of ammonia absorbed. Calcination strongly reduces the HAp total acidity (in μmol/g), mainly due to the loss of surface area, and to a lower extent, the specific acidity (in μmol/m$^2$).

The total acidity of the carboapatites is similar to the total acidity of the HAp-dried, and nearly four times higher than total acidity of the hydroxyapatite calcined at 900 °C. This suggests that, in some cases, the most important role in the acidity is played by the $Ca^{2+}$ ions. Literature data shows that hydroxyapatite presents anphoterous behavior, with Hammet constants ($H_0$) between +3.3 and +9.3 [3].

The specific acidity, however, shows a distinct pattern. Carboapatite A, that has $OH^-$ groups substituted by $CO_3^{2-}$, shows a specific acidity that is nearly four times higher than the acidity of the other samples. This distinct behavior may be caused by an increase in the number of $HPO_4^{2-}$ acid sites, resulting from replacement of the one $OH^-$ by $CO_3^{2-}$ group, required to counterbalance the ionic charges. However, this same replacement takes place on Carbo-B that presents low specific acidity. An alternative explanation for the increase in the specific acidity is due to thermal sintering during the calcination that would lead to more pronounced exposure of the *bc* and *ac* unit cell faces, and in consequence, the $Ca^{2+}$ ions become more exposed on the surface contributing more significantly to the solid specific acidity [26,27]. Accordingly, a five-fold increase in the average crystallite size, calculated by Scherrer [24], is observed between Carbo-A (1241 Å (0 0 *l*), 689 Å (*h k l*)) and Carbo-B (247 Å (0 0 *l*), 138 Å (*h k l*)).

The ammonia desorption profiles of the apatites are shown in Fig. 5. The strength of the acid sites is directly related to the desorption temperature, and for sake of analysis, ammonia is desorbed from weak acid sites below 300 °C, from moderately acid sites between 300 and 450 °C, from strong acid sites between 450 and 650 °C, and from very strong acid sites above 650 °C, for the heating rate of 10 °C/min. A complicating factor in the analysis of these profiles is that an ammonia salt is used in the preparation of the apatites. A blank test showed 10–20%

Table 2
Specific surface area ($S_{BET}$) and acidity by ammonia temperature-programmed desorption (TPD-$NH_3$) of the carboapatites and hydroxyapatite samples

| Samples | Thermal treatment | $CO_3^{2-}$ (%, w/w) | $S_{BET}$ (m$^2$/g) | Acidity ($NH_3$ ads.) | |
|---|---|---|---|---|---|
| | | | | Total (μmol/g) | Specific (μmol/m$^2$) |
| HAp-dried | 100 °C/24 h | – | 27 | 343 | 13 |
| HAp-calc | 900 °C/5 h | – | 10 | 81 | 8 |
| Carbo-A | 900 °C/5 h | 5.5 | 10 | 313 | 31 |
| Carbo-B | 400 °C/3 h | 12.5 | 41 | 315 | 8 |

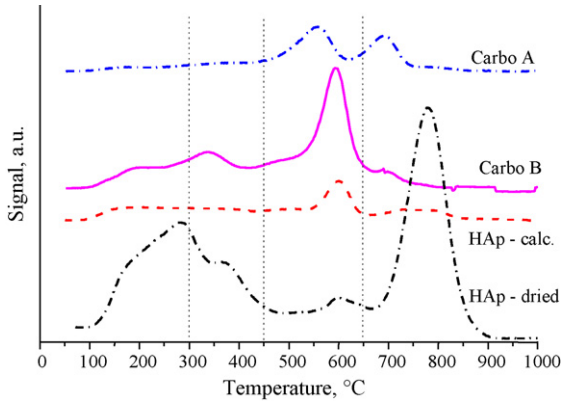


Fig. 5. Ammonia desorption profiles (TPD-$NH_3$) of the investigated apatites: HAp-dried; HAp-calc; Carbo-A; Carbo-B.

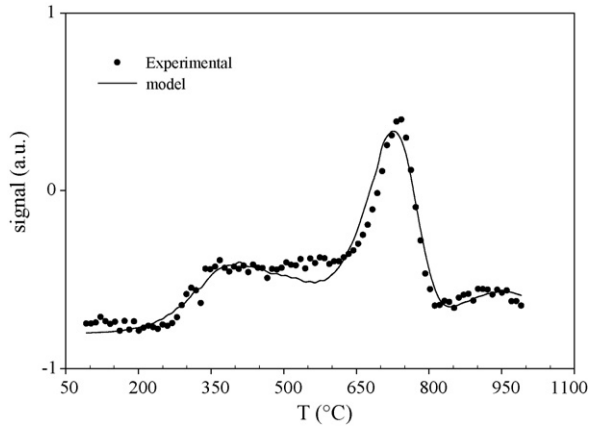


Fig. 6. Comparison between experimental and calculated ammonia desorption profiles (TPD-$NH_3$) of the dried hydroxyapatite (HAp-dried) at a heating rate of 5 °C/min.

of the ammonia desorbed comes from the solid itself, mainly at temperatures above 700 °C.

The effect of the thermal treatment in the distribution of acid sites is evident, the calcined sample presents a significant amount of strong acid sites and a smaller amount of very strong acid sites, while the non-calcined sample (HAp-dried) shows a broad distribution of acid sites excluding the strong ones, and the profile has a distinct valley from 500 to 700 °C (Fig. 5). The transformation of the weak acid sites to strong acid sites is attributed to the water desorption from the solid surface, while the strongly acid sites disappear due to dehydration of the $HPO_4^{2-}$ groups.

The Carbo-B shows two peaks of weak and moderately acidic sites in a lower relative amount than the dried hydroxyapatite (Fig. 5). There is a large peak in the strong acid sites region (450–650 °C) and practically no desorption peak was observed above 700 °C.

Carbo-A shows two very distinct peaks, resembling the HAp-dried sample, however, these peaks are associated to strong and very strong acid sites while the HAp-dried sample shows a broader acid site distribution with weak and very strong acid sites. The final result of the acid site distribution in Carbo-A is interesting, as despite of loosing weak acid sites, the total acidity remains the same.

Analyzing the data in Fig. 5 along with the structural features in Fig. 1, it is possible to associate the existence of the strong acid sites (450–650 °C) to the triangles of $Ca^{2+}$ ions present in all samples. The very strong acid sites can be attributed to the protons from $HPO_4^{2-}$ group and the weak acid sites to adsorbed water that interacts with ammonia through dipolar interactions.

Quantitative studies analyzing the TPD profiles of the HAp-calc through mathematical modeling of the desorption process [28] were able to identify four different ammonia adsorption sites, as defined in this study, in the HAp-dried sample with molar fractions 0.48, 0.28, 0.18 and 0.06; apparent activation energies for desorption of 38, 63, 125 and 146 kJ/mol, therefore ranging from weak to strong acid sites (Fig. 6). This wide range of acid sites seems to be present in all samples (Fig. 5) in different proportions, and shows that anion substitution is able to tune the surface properties of the material.

## 4. Conclusions

The synthesized apatites showed very distinctive acid sites strength and distribution, depending on the substitution and the thermal treatment. The substitution at the A sites $(OH)^-$, Carbo-A, leads to a three-fold increase in the total acidity and a significant change in the acid site distribution. Nevertheless, the substitution at B sites $PO_3^{3-}$, does not lead to significant change, highlighting the importance of the $Ca^{2+}$ ions on the acid properties of the material.

The total acidity measurement showed that the solid overall acidity is similar for the Carbo-A, Carbo-B and HAp-dried. Nevertheless, the TPD profiles showed significant differences in the acid strength distribution of these materials. This implies that the surface acidity of hydroxyapatites can be tuned to reach catalyst or adsorbent design criteria without changing the solid total acidity.

## Acknowledgement

The authors wish to thank CNPq and FAPERJ for the financial support.

## References

[1] Y. Takeuchi, H. Arai, J. Chem. Eng. Jpn. 22 (1) (1990) 75–80.
[2] A. Aklil, M. Mouflih, S. Sebti, J. Hazard. Mater. 112 (3) (2004) 183–190.
[3] H. Monma, J. Catal. 75 (1982) 200–203.
[4] C.L. Kibby, S. Lande, W. Hall, J. Am. Chem. Soc. 94 (1972) 214.
[5] C.L. Kibby, W.K. Hall, J. Catal. 31 (1) (1973) 65–73.
[6] Y. Izumi, S. Sato, K. Urabe, Chem. Lett. (1982) 415.
[7] Y. Matsumura, J. Moffat, J. Catal. 148 (1) (1994) 323–333.
[8] Y. Matsumura, J. Moffat, J. Chem. Soc., Faraday Trans. 92 (1996) 1981.
[9] J.H. Jun, T.-J. Lee, T.H. Lim, S.-W. Nam, S.-A. Hong, K.J. Yoon, J. Catal. 221 (1) (2004) 178–190.
[10] Z. Opre, J.-D. Grunwaldt, M. Maciejewski, D. Ferri, T. Mallat, A. Baiker, J. Catal. 230 (2005) 406–419.
[11] S. Sebti, R. Tahir, R. Nazih, A. Saber, S. Boulaajaj, Appl. Catal. A: Gen. 228 (1–2) (2002) 155–159.
[12] F. Bazi, H. El Badaoui, S. Tamani, S. Sokori, A. Solhy, D.J. Macquarrie, S. Sebti, Appl. Catal. A: Gen. 301 (2) (2006) 211–214.

[13] S. Sebti, R. Tahir, R. Nazih, S. Boulaajaj, Appl. Catal. A: Gen. 218 (1–2) (2001) 25–30.
[14] N. Cheikhi, M. Kacimi, M. Rouimi, M. Ziyad, L.F. Liotta, G. Pantaleo, G. Deganello, J. Catal. 232 (2) (2005) 257–267.
[15] S. Shimoda, T. Aoba, E. Morenoe, Y. Miake, J. Dent. Res. 69 (1990) 1731.
[16] J. Guerra-Lopez, R. Pomes, C.O. Della Vedova, R. Vina, G. Punte, J. Raman Spectrosc. 32 (2001) 255.
[17] St. Naray-Szabo, Zeitsch-Krist. 75 (1930) 323.
[18] C.A. Beevers, D.B. McIntyre, Miner. Mag. 27 (1945) 254.
[19] J.C. Elliott, Structure and Chemistry of the Apatites and Other Calcium Orthophosphates, Elsevier Science, Amsterdam, 1994.
[20] Y. Suetsugu, Y. Takahashi, F.P. Okamura, J. Tanaka, J. Solid State Chem. 155 (2000) 292–297.
[21] G. Bonel, Ann. Chim. (Paris) 7 (1972) 65–88, 127–144.
[22] T. Masuda, Y. Fujikata, H. Ikeda, S. Matsushita, K. Hashimoto, Appl. Catal. A 162 (1997) 29–40.
[23] R.M. Wilson, J.C. Elliott, S.E.P. Dowker, L.M. Rodriguez-Lorenzo, Biomaterials 26 (2005) 1317.
[24] G.K. Joshi, A.Y. Khot, C.R. Swaqnt, Solid State Commun. 65 (1988) 1593.
[25] A. Slósarczyk, Z. Paszkiewicz, C. Paluszkiewicz, J. Mol. Struct. 744–747 (2005) 657–661.
[26] K. Kandori, T. Shimizu, A. Yasukawa, T. Ishikawa, Colloid Surf. B: Biointerf. 5 (1995) 81–87.
[27] T. Kawasaki, S. Takahashi e, K. Ikeda, Eur. J. Biochem. 152 (1985) 351.
[28] M. Nele, G.F. Moreira, N.S. de Resende, V.M.M. Salim e, J.C.S. Pinto, anais do XIX Simpósio Iberoamericano de Catálise, 2004, p. 188.